

البحث العددي في الاهتزاز الديناميكي الجانبي لنظام عمود نقل الحركة في المضخة التوربينية

*ون-جي تشو، ***شيويه سونغ وي، *غوانغ-كوان وو، ***وان جيانغ ليو
و*لو تشين وانغ

*معهد المعدات التكنولوجية، جامعة تشجيانغ، وهانغتشو، الصين.

**كلية الهندسة، معهد كيوشو للتكنولوجيا، كيتاكيوشو، اليابان.

***معهد هارين للآلات الكهربائية الكبيرة، هارين، الصين.

الخلاصة

هذا البحث يقدم نموذج الاهتزاز الديناميكي جديد لنظام عمود نقل الحركة في المضخة التوربينية باعتماد قوى عزل السائل الغير الخطية، بالإضافة إلى الأثر المزدوج للسحب المغناطيسي الغير متوازن، وتوجيه قوة تحمل، وقوة الكتلة غير متوازنة والقدرة الهيدروليكية. وتستند الحسابات على طريقه العناصر المحددة ومعادلة لاغرانج. وتم تقسيم وتطوير العقدة آليا وذلك عن طريق تقسيم العقدة بسرعة ودقة. وتم ذلك من خلال حل المعادلات التفاضلية للحركة والاستجابة الديناميكية للوحدة عن طريق أسلوب نيومارك الضمني. وتم بحث الخصائص الديناميكية غير الخطية من قوة العزل التاجي للسائل. وتم تحليل الاهتزازات الجانبية المتغيرة مع الزمن وثابتة من ثلاثة اتجاهات باستخدام الرسوم البيانية والاستجابة الدورية ومدارات محور ثابتة والرسوم البيانية. وتبين النتائج بأن إنحراف العمود وعازل السوائل وطول فجوة الهواء كان لها آثار كبيرة على الاهتزاز الديناميكي لنظام عمود نقل الحركة. الانحراف العمود كان 0 ملم، وإزالة عازل السوائل كان 3 ملم، وطول فجوة الهواء كان 35 ملم، واستقرار النظام كان الأعلى. والنتائج الكمية والنوعية هي ذات صلة للاستخدام الهندسي في تصميم نظام عمود نقل الحركة في المضخة التوربينية.

Numerical research on dynamic lateral vibration of a pump-turbine's shaft system

Wen-Jie Zhou*, Xue-Song Wei***, Guang-Kuan Wu*, Wan-Jiang Liu*** and Le-Qin Wang*

**Institute of Process Equipment, Zhejiang University, Hangzhou, China*

***Faculty of Engineering, Kyushu Institute of Technology, Kitakyushu, Japan*

****Harbin Institute of Large Electrical Machinery, Harbin, China*

**Corresponding author: zhouwenjiezwj@zju.edu.cn*

ABSTRACT

The novel transient dynamic vibration model of pump-turbine's shaft system considers nonlinear seal fluid forces, in addition to the coupled effects of unbalanced magnetic pull (UMP), guide bearing force, unbalanced mass force and hydraulic force. The calculations are based on the finite element method (FEM) and Lagrange equation. Node automation division method (NADM) is developed in-house for quick and accurate node division. The differential equations of motion and the dynamic response of the unit are resolved by implicit Newmark method. The nonlinear dynamic characteristics of crown seal force and UMP are researched. The transient and steady lateral vibrations of three bearings are also analyzed using the periodic response diagrams, steady axis orbits and waterfall diagrams. The calculated results demonstrate that the mounted eccentricity, crown seal channel clearance and air-gap length have significant effects on the dynamic vibration of the shaft system. When the mounted eccentricity is 0mm, clearance of crown seal is 3mm, air-gap length is 35mm, the stability of the system is the highest. Both quantitative and qualitative results are relevant for engineering use in pump-turbine's shaft system design.

Keywords: Finite element method (FEM); Newmark method; node automation division method (NADM); transient nonlinear seal forces.

NOMENCLATURE

b	Clearance of Crown Seal
e	Eccentricity Ratio
e_m	Mounted eccentricity
f	Frequency
g	Gravitational Acceleration

I_j	Excitation Current
k_j	Fundamental MMF Coefficient
l	Length of Crown Seal
L	Length of Generator Rotor
P	Pressure in Crown Seal
P_{inlet}	Inlet Pressure of Crown Seal
P_{outlet}	Outlet Pressure of Crown Seal
Q	Generalized Forces
Q_f	Flow in Crown Seal
r	Radius of Crown Seal
R	Radius of Generator Rotor
T	Kinetic Energy
U	Independent Generalized Coordinates
V	Strain Energy
x	x-direction in Cross Section
y	y-direction in Cross Section
z	Axial Direction
δ	Eccentric Distance
δ_0	Air-gap Length
Δp	Pressure Drop in Crown Seal
ε	Relative Eccentricity
θ	Rotation Angle
λ	Friction Factor
μ	Flow Coefficient of Crown Seal
μ_0	Air Permeance
ρ	Density
Ω	Rotor Speed
Ω_{rated}	Rated Rotor Speed

Subscript

BS	Band Seal Force
CS	Crown Seal Force

e	Elastic Shaft Element
g	Generator Rotor
i	ith Channel
LGB	Lower Guide Bearing Force
r	Runner
TGB	Turbine Guide Bearing Force
UGB	Upper Guide Bearing Force
UH	Unbalance Hydraulic Force
UM_Rotor	Unbalance Mass Force of Generator Rotor
UM_Runner	Unbalance Mass Force of Runner

INTRODUCTION

The vibration state of pump-turbine's shaft system not only affects the units work efficiency, but also affects the life span of the units. An excessive vibration can cause fatigue damage to the rotating machinery and or cause a catastrophic damage (Muszynska, 2005). In view of this, an accurate dynamic vibration model of pump-turbine's shaft system is essential. In fact, the rotor vibration model responses to a variety of factors, such as bearing effect, generator's rotor electromagnetic force, turbine runner's unbalanced force etc. In order to accurately predict the vibration status of pump-turbine's shaft system, the combined effect of various factors must be taken into consideration.

Many researchers have made a lot of material contribution to the improvement of the sealing model. The finite-length method proposed by Childs (1983), was widely applied to calculate the annular fluid seal force in the rotor-bearing-seal system. The two-control-volume analysis for the rotor dynamics' coefficients of labyrinth seals presented by Wyssmann *et al.* (1984) and Scharrer (1988), was used as a theoretical foundation for calculating dynamic characteristics of the complex seal structures. The computational fluid dynamics (CFD) software was used to calculate the coefficients and internal flow state of the labyrinth seals. Yan *et al.* (2011) selected a range of step height-to-clearance ratios and step axial position-to-pitch ratios to numerically investigate the influence of the sealing clearance and step geometries on the leakage flow and heat transfer coefficients of stepped labyrinth seals. Li *et al.* (2009) applied the numerical simulations for investigating the sealing performance and flow pattern of brush seals, and found that the brush seals displayed better leakage performance than the referenced labyrinth seal on the condition of zero clearance size.

The effects of the guide bearings and UMP were also researched in the past. The new form of the Reynolds equation, which contained the film thickness, the squeeze

motion of the journal and the rotation motion of the pad, was derived by Peng *et al.* (2007). Based on the equation, the dynamic features of water guide bearing used in the Gezhouba 10 F hydro-generator unit were numerically researched. Simmons *et al.* (2014) experimentally researched the steady state and dynamic characteristics of the guide bearings by varying the oil film thickness, pad loading and the oil temperature. Concerning the UMP, Peters *et al.* (2007) calculated the UMP of a hydropower generator with 20% static eccentricity for various no-load voltages and loads and discovered that there was a close relationship between the UMP and saturation. Guo *et al.* (2002) theoretically calculated the UMP in a three-phase generator under no-load, and derived the analytical expression for the UMP. The research results illustrated that UMP played an important role on the vibration characteristics of the rotor system.

The recent background researches on the shaft's vibrations are the following. The shaft models of the pump-turbine and the hydraulic turbine are very similar. De Jaeger *et al.* (1994) proposed a nonlinear dynamic model of hydro turbines and demonstrated that the simulation results of the model had the accuracy as high as the load rejections. Feng & Chu (2001) established a model of a large water-turbine generator set, the critical speed and vibration modes by the RTMM were calculated. The lateral vibration model including the effects of rotor geometry, guide bearing forces and magnetic forces, and so on was presented by Bettig & Han (1999); it was inaccurate due to the defects of the guide bearing model. Xu *et al.* (2011) and Xu & Li (2012) put forward a brief and practical database method to model the guide bearing. Bai *et al.* (2012) calculated the multiple critical speeds and modal vibration shapes of a hydro-turbine's rotor system using ANSYS software, and pointed out that gyroscopic effect should be considered to ensure the accuracy of the calculation. Lai *et al.* (2012) researched the influences of the guide bearing with varying support stiffness on the lateral vibration's characteristics of a Francis turbine generator unit.

In present work, the shaft system vibration model of pump-turbine is improved. Previous models of hydraulic turbine units included the three guide bearing forces, unbalanced magnetic pull, hydraulic force and unbalanced forces. However, another important factor, the nonlinear sealing force, was completely ignored in the calculation process. Gong *et al.* (2013, 2014) found that the sealing affects the stability of the hydraulic turbine system and pointed out that the sealing force should be taken into account when solving the dynamic characteristics of hydraulic turbine shaft system.

In this paper, a novel transient vibration model of pump-turbine's shaft system is established based on the FEM. This model accounts the UMP, guide bearings forces, three-channel sealing force, Muszynska nonlinear fluid force and unbalanced forces. The nonlinear relationships between crown seal force and UMP with related parameters are researched. The NADM is also applied to ensure that the finite element nodes are divided quickly and accurately. The implicit Newmark numerical method is adopted

to determine the vibration state. The transient and steady vibration characteristics of a pump-turbine's shaft system at the positions of three guide bearings are presented.

MODEL OF THE PUMP-TURBINE'S SHAFT SYSTEM

The simplified model of the pump-turbine's shaft system is shown in Figure 1. In fact, the pump-turbine is a complicated coupled system including multiple components and it is difficult and unnecessary to take all factors into consideration; then the original model is simplified. The dynamic lateral vibration state of the pump-turbine's shaft system is mainly determined by the coupling effects of guide bearings, rotor of generator, runner and the seal structures described below.

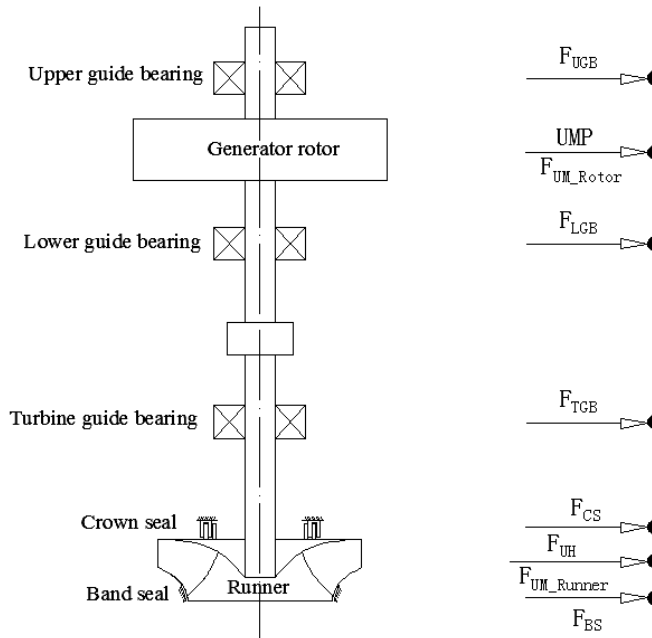


Fig. 1. Simplified model of pump-turbine's shaft system

The generator's rotor and the runner, are replaced by the lumped mass points with the moment of inertia. The guide bearing force and sealing fluids force also act on these lumped points. The first guide bearing force acting on the rotor system is F_{UGB} , which is followed by F_{LGB} and F_{TGB} in the axial direction. The forces acting on the lumped points of generator's rotor are UMP and F_{UM_Rotor} , and the forces acting on the lumped points of the runner are F_{UH} and F_{UM_Runner} . The sealing fluids' forces of the crown seal with the three-channel structure and the band seal are F_{CS} and F_{BS} .

COMPONENT MODELS AND SYSTEM MOTION EQUATIONS

The pump-turbine's shaft system has a multi-degree of freedom and is a non-conservative system. The FEM and the Lagrange equation solve the motion equations of the system. A combination of FEM and NADM is a precise instrument for numerical calculation of the current model. The concrete steps of NADM are summarized below (see Figure 5 for reference):

Step 1: Completing the shaft node division based on maximum node spacing, and sorting the node numbers from the generator shaft's top end to the pump's bottom end.

Step 2: Inserting the generator rotor and runner nodes, and rearranging the previous node numbers according to the position on the shaft.

Step 3: Saving the new node locations of the shaft assembly.

Step 4: Inserting the three guide bearing nodes, and rearranging the node numbers including the new nodes and saving the new node locations.

Step 5: Inserting the crown node and the band node, rearranging the node numbers and saving the node locations containing all the components.

In addition to automation, the NADM is modular, i.e. the node numbers are automatically divided according to the components that were included.

Model of generator rotor, runner and pump-turbine shaft

The modeling process of generator rotor, runner and pump-turbine shaft is similar to modeling of multistage rotor system (Zhou *et al.*, 2014). The Lagrange equation of non-conservative system is described as follows:

$$\frac{d}{dt} \left(\frac{\partial T}{\partial \dot{\mathbf{u}}} \right) - \frac{\partial (T - V)}{\partial \mathbf{u}} = \mathbf{q} \quad (1)$$

The generator's rotor degrees of freedom (DOF) contain two translational displacements: x , y ; and two rotational displacements: θ_x , θ_y , therefore

$$\mathbf{u}_{g-x} = [x, \theta_y]^T, \mathbf{u}_{g-y} = [y, -\theta_x]^T$$

The strain energy of generator's rotor is ignored and the kinetic energy is expressed as following:

$$T_g = \frac{1}{2} \dot{\mathbf{u}}_{g-x}^T \mathbf{M}_g \dot{\mathbf{u}}_{g-x} + \frac{1}{2} \dot{\mathbf{u}}_{g-y}^T \mathbf{M}_g \dot{\mathbf{u}}_{g-y} + \Omega \dot{\mathbf{u}}_{g-x}^T \mathbf{J} \dot{\mathbf{u}}_{g-y} + \frac{1}{2} \mathbf{J}_g \Omega^2 \quad (2)$$

The motion equations of generator's rotor are obtained by substituting the Equation (2) into the equation (1):

$$\begin{cases} \mathbf{M}_g \ddot{\mathbf{u}}_{g_x} + \Omega \mathbf{J} \dot{\mathbf{u}}_{g_y} = \mathbf{q}_{g_x} \\ \mathbf{M}_g \ddot{\mathbf{u}}_{g_y} - \Omega \mathbf{J} \dot{\mathbf{u}}_{g_x} = \mathbf{q}_{g_y} \end{cases} \quad (3)$$

The modeling process of a runner is the same as for the generator's rotor. The motion equations of the runner:

$$\begin{cases} \mathbf{M}_r \ddot{\mathbf{u}}_{r_x} + \Omega \mathbf{J} \dot{\mathbf{u}}_{r_y} = \mathbf{q}_{r_x} \\ \mathbf{M}_r \ddot{\mathbf{u}}_{r_y} - \Omega \mathbf{J} \dot{\mathbf{u}}_{r_x} = \mathbf{q}_{r_y} \end{cases} \quad (4)$$

Figure 2 shows the elastic shaft element of pump-turbine shaft containing two endpoints A and B. The generalized coordinates are defined:

$$\mathbf{u}_{e_x} = [x_A, \theta_{yA}, x_B, \theta_{yB}]^T, \mathbf{u}_{e_y} = [y_A, -\theta_{xA}, y_B, -\theta_{xB}]^T$$

In fact, the generalized coordinates of A and B are expressed by these two endpoints. The kinetic energy and strain energy of the element is calculated by integrating over the length of the element:

$$T_e = \frac{1}{2} \dot{\mathbf{u}}_{e_x}^T (\mathbf{M}_{eT} + \mathbf{M}_{eR}) \dot{\mathbf{u}}_{e_x} + \frac{1}{2} \dot{\mathbf{u}}_{e_y}^T (\mathbf{M}_{eT} + \mathbf{M}_{eR}) \dot{\mathbf{u}}_{e_y} + \Omega \dot{\mathbf{u}}_{e_x}^T \mathbf{J} \dot{\mathbf{u}}_{e_y} + \frac{1}{2} j_{pe} \cdot l \cdot \Omega \quad (5)$$

$$V_e = \frac{1}{2} \mathbf{u}_{e_x}^T \mathbf{K}_e \mathbf{u}_{e_x} + \frac{1}{2} \mathbf{u}_{e_y}^T \mathbf{K}_e \mathbf{u}_{e_y} \quad (6)$$

The motion equations of the elastic shaft element is obtained by substituting Equations (5) and (6) into Equation (1):

$$\begin{cases} \mathbf{M}_e \ddot{\mathbf{u}}_{e_x} + \Omega \mathbf{J} \dot{\mathbf{u}}_{e_y} + \mathbf{K}_e \mathbf{u}_{e_x} = \mathbf{q}_{e_x} \\ \mathbf{M}_e \ddot{\mathbf{u}}_{e_y} - \Omega \mathbf{J} \dot{\mathbf{u}}_{e_x} + \mathbf{K}_e \mathbf{u}_{e_y} = \mathbf{q}_{e_y} \end{cases} \quad (7)$$

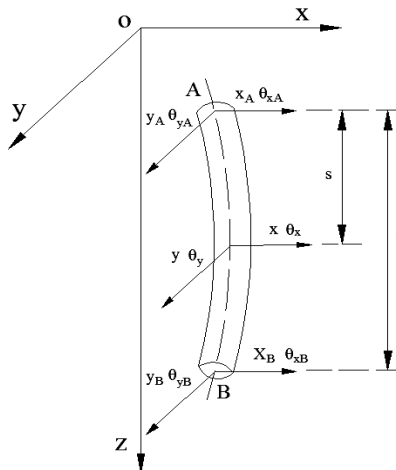


Fig. 2. Elastic shaft element

Model of the crown seal and the band seal

Three-channel sealing structure is often used in crown seal because of its good sealing characteristics. Figure 3(a) and Figure 3(b) show the unilateral shaft section and a cross section of the three-channel sealing structure, respectively.

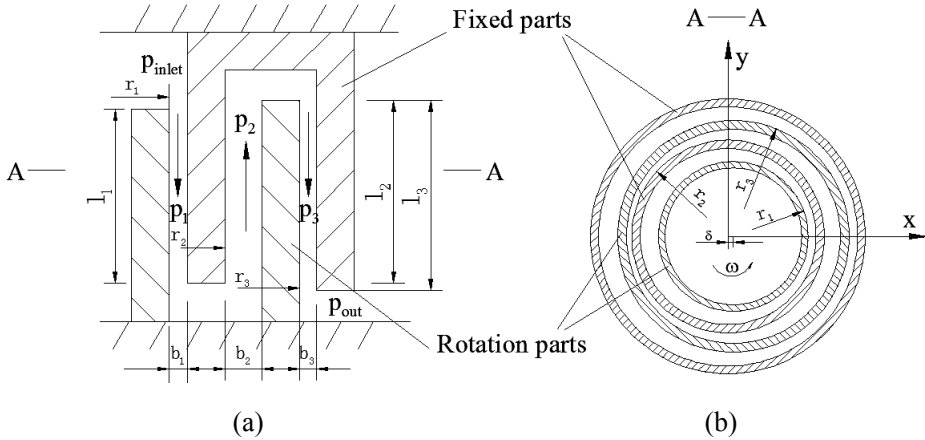


Fig. 3. Three-channel sealing structure

From the Figure 3, it is seen that when the rotation parts offset δ to the right, the clearance size of the first and third channel reduces, and, on the contrary, the clearance size of the second channel increases. Actually, the pressure drop in each channel is not only related to the offset value, but also to the circumferential angle. The function of pressure drop in each channel is given as follows (Wang *et al.*, 2011):

$$\frac{\Delta p_i(\theta, \delta)}{\rho g} = \frac{1}{2g} \frac{1}{[\mu_i(\theta, \delta) b_i(\theta, \delta) r_i]^2} \left(\frac{dQ_f}{d\theta} \right)^2 \quad i = 1, 2, 3 \quad (8)$$

The flow coefficient for all channels:

$$\frac{1}{\mu(\theta, \delta)} = \sqrt{\sum_{i=1}^3 \frac{1}{\mu_i(\theta, \delta) \left[\frac{r_i b_i(\theta, \delta)}{r_i b_i(\theta, \delta)} \right]^2}} \quad (9)$$

Adding the pressure drop in each channel and combining the Equation (8) with Equation (9), gives:

$$\frac{P_{inlet} - P_{out}}{\rho g} = \frac{1}{2g} \left[\frac{1}{\mu(\theta, \delta) b_i(\theta, \delta) r_i} \right]^2 \left(\frac{dQ_f}{d\theta} \right)^2 \quad (10)$$

According to the Equations (8) and (10), the pressure drop in each channel is expressed as the function of δ and θ :

$$\Delta p_i(\theta, \delta) = (p_{inlet} - p_{out}) \left[\frac{\bar{\mu}(\theta, \delta)}{\mu_i(\theta, \delta)} \right]^2 \left[\frac{b_1(\theta, \delta)}{b_i(\theta, \delta)} \right]^{-2} \left(\frac{r_1}{r_i} \right)^2 \quad i = 1, 2, 3 \quad (11)$$

Furthermore, the pressure in each channel is described as follows:

$$\begin{cases} p_1(z, \theta, \delta) = p_{inlet} - \Delta p_1(\theta, \delta) + \Delta p_1(\theta, \delta) \frac{\lambda z_1}{2b_1(\theta, \delta) + \lambda l_1} \\ p_2(z, \theta, \delta) = p_{out} + \Delta p_3(\theta, \delta) + \Delta p_2(\theta, \delta) \frac{\lambda z_2}{2b_2(\theta, \delta) + \lambda l_2} \\ p_3(z, \theta, \delta) = p_{out} + \Delta p_3(\theta, \delta) \frac{\lambda z_3}{2b_3(\theta, \delta) + \lambda l_3} \end{cases} \quad (12)$$

Taking the δ as an independent variable, the force in each channel is calculated through computing an integral over the length of the channel:

$$F_i(\delta) = \int_0^{l_i} dz_i \int_0^{2\pi} p_i(z, \theta, \delta) \cos\theta_i r_i d\theta \quad (13)$$

Therefore, the total crown sealing force with three-channel structure is:

$$F_{CS} = \sum_{i=1}^3 (-1)^{i-1} \int_0^{l_i} dz_i \int_0^{2\pi} p_i(z, \theta, \delta) \cos\theta_i r_i d\theta \quad (14)$$

The Muszynska nonlinear seal force model is commonly used for the band seal. Muszynska (1988) and Muszynska & Bently (1990) proposed a classic nonlinear seal fluid dynamic force model, regarding the circulating velocity as the key factor of the stability in the seal structure. The model has been widely used to describe the nonlinear characteristic of the seal force and it is expressed as follows:

$$\begin{Bmatrix} F_{BS-x} \\ F_{BS-y} \end{Bmatrix} = \begin{bmatrix} K_{bs} - m_{bs} \gamma^2 \Omega^2 & \gamma \Omega C_{bs} \\ -\gamma \Omega C_{bs} & K_{bs} - m_{bs} \gamma^2 \Omega^2 \end{bmatrix} \begin{Bmatrix} x \\ y \end{Bmatrix} - \begin{bmatrix} C_{bs} & 2m_{bs} \gamma \Omega \\ -2m_{bs} \gamma \Omega & C_{bs} \end{bmatrix} \begin{Bmatrix} \dot{x} \\ \dot{y} \end{Bmatrix} - \begin{bmatrix} m_{bs} & 0 \\ 0 & m_{bs} \end{bmatrix} \begin{Bmatrix} \ddot{x} \\ \ddot{y} \end{Bmatrix} \quad (15)$$

Where the values of K_{bs} , γ and C_{bs} (the nonlinear function of disturbance displacement) present the obvious nonlinear characteristics. The coefficient values and calculating process are given by Gong *et al.* (2013).

Model of other components

According to the calculating method of UMP proposed by Guo *et al.* (2002), the unbalance magnetic pull would be produced when the clearance between the rotor and stator is not homogeneous. The generator pole numbers in pump-turbine are always larger than 3, therefore the UMP is evaluated approximately by the following formula:

$$UMP_x = f_1 \cos\theta, UMP_y = f_1 \sin\theta \quad (16)$$

Where

$$f_1 \approx \frac{RL\pi\mu_0 I_j^2 k_j^2}{\delta_0^2} \left(\frac{1}{2}\varepsilon + \frac{5}{8}\varepsilon^3 \right) \tag{17}$$

The upper, lower and turbine guide bearings, are another important factor influencing the lateral vibration characteristics. In this paper, the stiffness of the guide bearings is set to 1×10^9 . The effect of unbalanced hydraulic force is reduced to the constant hydraulic force and the periodic hydraulic force. The former is a constant value in a fixed direction, and the latter is a periodic changes due to changing of the rotor speed and the runner rotating moment.

Motion equations of pump-turbine’s shaft system

Combining the motion equations of the elastic shaft element, generator’s rotor and the runner, the motion equation of pump-turbine’s shaft system is obtained (Zhong *et al.*, 1987):

$$\begin{cases} [M']\{\ddot{U}_1\} + \Omega[J']\{\dot{U}_2\} + [K']\{U_1\} = \{Q_1\} \\ [M']\{\ddot{U}_2\} - \Omega[J']\{\dot{U}_1\} + [K']\{U_2\} = \{Q_2\} \end{cases} \tag{18}$$

Where

$$\begin{cases} \{U_1\} = [x_1, \theta_{y1}, x_2, \theta_{y2} \cdots x_N, \theta_{yN}]^T \\ \{U_2\} = [y_1, -\theta_{x1}, y_2, -\theta_{x2} \cdots y_N, -\theta_{xN}]^T \end{cases}$$

In fact, the external forces, Q_1 and Q_2 , are mainly caused by the unbalanced mass of generator’s rotor and the runner. The above motion equation is improved by considering the guide bearing force, UMP, crown seal and band seal forces, etc. Therefore, the motion Equation (18) is read:

$$\begin{bmatrix} M' & \\ & M' \end{bmatrix} \begin{Bmatrix} \ddot{U}_1 \\ \ddot{U}_2 \end{Bmatrix} + \begin{bmatrix} & \Omega[J'] \\ -\Omega[J'] & \end{bmatrix} \begin{Bmatrix} \dot{U}_1 \\ \dot{U}_2 \end{Bmatrix} + \begin{bmatrix} K' & \\ & K' \end{bmatrix} \begin{Bmatrix} U_1 \\ U_2 \end{Bmatrix} = \begin{Bmatrix} F_{UM_x} + F_{CS_x} + F_{BS_x} + F_{GB_x} + UMP_x + F_{UH_x} \\ F_{UM_y} + F_{CS_y} + F_{BS_x} + F_{GB_y} + UMP_y + F_{UH_y} \end{Bmatrix} \tag{19}$$

Simplifying the above motion equation gives:

$$[M] = \begin{bmatrix} M' & \\ & M' \end{bmatrix}; [C] = \begin{bmatrix} & \Omega[J'] \\ -\Omega[J'] & \end{bmatrix}; [K] = \begin{bmatrix} K' & \\ & K' \end{bmatrix}$$

$$\{U\} = \begin{Bmatrix} U_1 \\ U_2 \end{Bmatrix}; \{Q\} = \begin{Bmatrix} F_{UM_x} + F_{CS_x} + F_{BS_x} + F_{GB_x} + UMP_x + F_{UH_x} \\ F_{UM_y} + F_{CS_y} + F_{BS_x} + F_{GB_y} + UMP_y + F_{UH_y} \end{Bmatrix}$$

The most simplified motion equation of pump-turbine’s shaft system is described in the following form:

$$[M]\{\ddot{U}\} + [C]\{\dot{U}\} + [K]\{U\} = \{Q\} \tag{20}$$

CALCULATING METHOD OF THE MOTION EQUATION

The scale of motion equation is associated with the node numbers, which means the solving difficulty and time will increase as the numbers of node increase. For the nonlinear equations, the unconditional convergence Newmark implicit integral method, which can obtain better precision and computing speed, is applied to solve the dynamic lateral vibration of a pump-turbine's shaft system. The iterative form of the Newmark implicit method is shown below (Gong *et al.*, 2014):

$$\left(K + \frac{1}{\sigma \Delta t^2} M + \frac{\beta}{\sigma \Delta t} C \right) U_{t+\Delta t} = Q_{t+\Delta t} + M \left[\frac{1}{\sigma \Delta t^2} U_t + \frac{1}{\sigma \Delta t} \dot{U}_t + \left(\frac{1}{2\sigma} - 1 \right) \ddot{U}_t \right] + C \left(\frac{\beta}{\sigma \Delta t} U_t + \left(\frac{\beta}{\sigma} - 1 \right) \dot{U}_t + \frac{\Delta t}{2} \left(\frac{\beta}{\sigma} - 2 \right) \ddot{U}_t \right) \tag{21}$$

$$\ddot{U}_{t+\Delta t} = \frac{1}{\sigma \Delta t^2} (U_{t+\Delta t} - U_t) - \frac{1}{\sigma \Delta t} \dot{U}_t - \left(\frac{1}{2\sigma} - 1 \right) \ddot{U}_t \tag{22}$$

$$\dot{U}_{t+\Delta t} = \dot{U}_t + (1 - \beta) \Delta t \ddot{U}_t + \beta \Delta t \ddot{U}_{t+\Delta t} \tag{23}$$

Where

$$\sigma = 1/4, \beta = 1/2$$

From the iterative form, it is seen that the displacement, velocity and acceleration at $t+\Delta t$ is calculated, if only the corresponding values from the previous time step are given. In fact, some external forces on the shaft system, such as the F_{BS} and UMP, are determined by their nodes displacement and velocity. Thus, the internal loop iterations are adopted to solve this problem. The solving process for concrete dynamic lateral vibration of the pump-turbine's shaft system is shown in Figure 4.

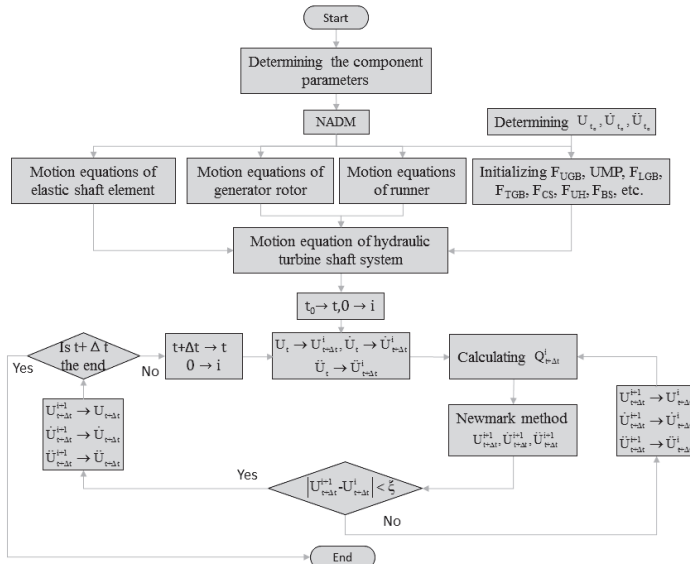


Fig. 4. Flow chart of dynamic lateral vibration solving process

In the present research, a pump-turbine pumped storage units is adopted. The CAD model of this pump-turbine rotor system is shown in Figure 5(a), the corresponding finite element model and node numbers are shown in Figure 5(b). The shaft system is divided into 15 nodes and 14 sections. The nonlinear forces from the crown seal and band seal are imposed on the node 12 and node 15, respectively. The main parameters of each shaft section are listed in Table 1. The calculating coefficients of the band seal are in accordance with Gong *et al.* (2013) and the other main parameters used in the calculation are listed in Table 2.

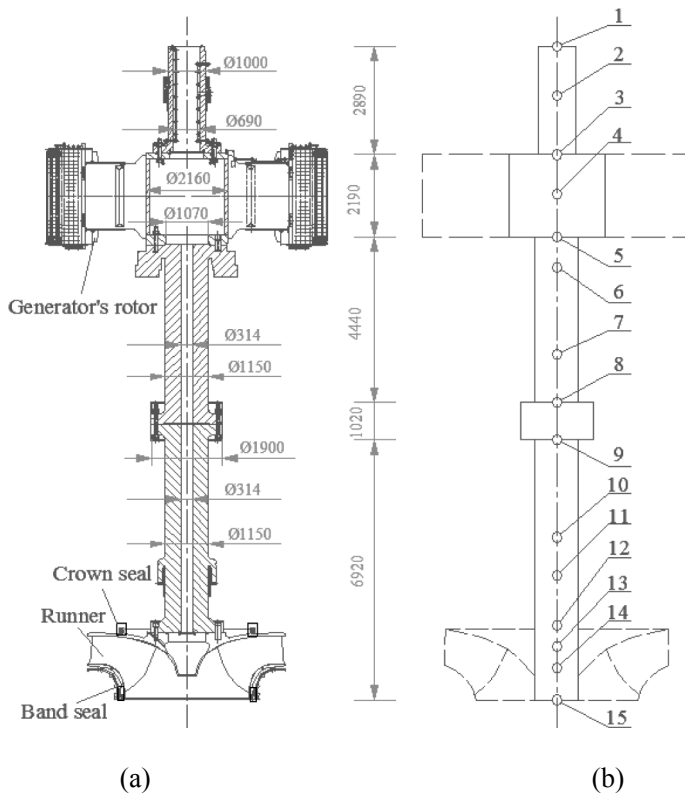


Fig. 5. The real model (a) and the finite element model (b) of the pump-turbine's shaft system, where nodes with corresponding numbers are referred to: 1 - generator's upper shaft end; 2 - upper guide bearing; 3 - upper generator's coupling; 4 - generator's rotor; 5 - lower generator's coupling; 6 - lower guide bearing; 7 - generator's lower shaft; 8 - coupling from the generator's shaft side; 9 - coupling from the runner's shaft side; 10 - runner's upper shaft; 11 - turbine guide bearing; 12 - crown seal; 13 - runner; 14 - runner; 15 - band seal

Table 1. Main parameters of each shaft section

No. of section	Section length (mm)	Inside diameter (mm)	Outside diameter (mm)	Section mass (kg)
1	2890	690	1000	9275.4
2	2190	1070	2160	47234.3
3	4440	314	1150	33290.1
4	1020	314	1900	21941.5
5	6920	314	1150	51884.5

Table 2. Main parameters of other components

m_g (kg)	344000	r_1 (m)	1.71	P_{inlet} (kPa)	1500
m_r (kg)	55000	r_2 (m)	1.74	P_{outlet} (kPa)	1000
e_g (m)	0.0001	r_3 (m)	1.77	μ_0	$4*\pi*10^{-7}$
e_r (m)	0.0001	b_1 (m)	0.002	I_j (A)	1824.1
l_1 (m)	0.007	b_2 (m)	0.002	δ_0 (m)	0.035
l_2 (m)	0.007	b_3 (m)	0.002	R (m)	3.75
l_3 (m)	0.007	g (m/s ²)	9.8	L (m)	2.12
Ω_{rated} (r/min)	250				

NUMERICAL RESULTS AND DISCUSSIONS

The dynamic lateral vibration characteristics of pump-turbine's shaft system were researched. Figure 6 shows the dynamic relationship of F_{CS} with eccentricity ratio in different channel clearance and channel length. It can be seen that F_{US} increases with the increase of eccentricity ratio and channel length, especially for the higher values. However, the larger channel clearance will cause smaller F_{CS} .

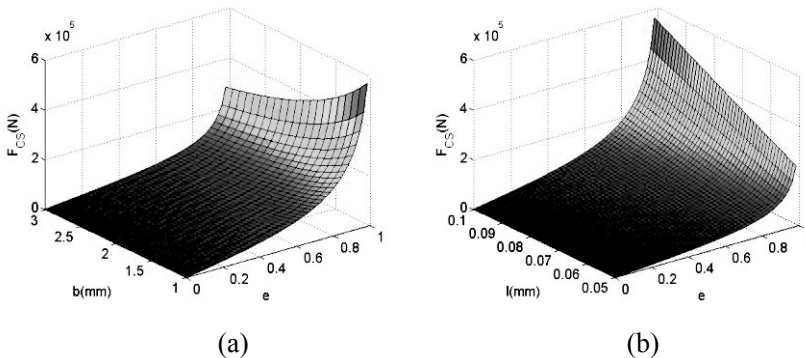


Fig. 6. The change of F_{CS} with eccentricity ratio and (a) channel clearance, (b) channel length

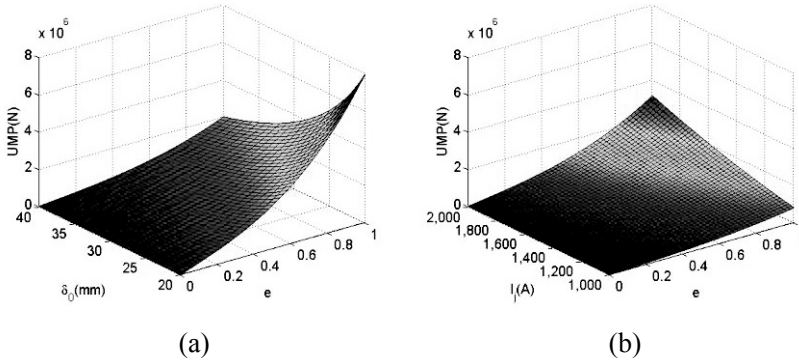


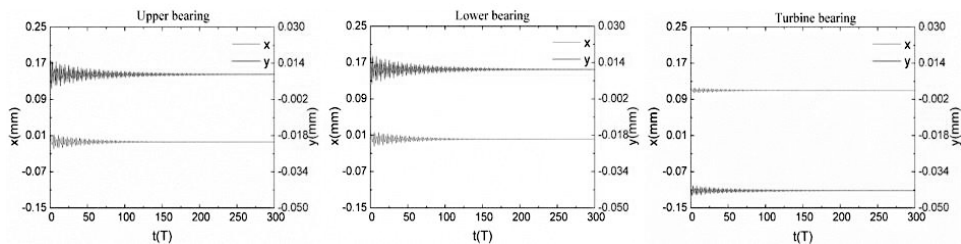
Fig. 7. The change of UMP with eccentricity ratio and (a) air-gap length, (b) excitation current

The impact of air-gap length and excitation current on UMP is shown on Figure 7. Like the effect of channel’s clearance and length on F_{US} , the narrower air-gap length and higher excitation current cause larger UPM, which increases as eccentricity ratio increases. More importantly, from Figure 6 and Figure 7, it is seen that the changes of F_{CS} and UMP present nonlinear trends in the change of related parameters.

Effect of the mounted eccentricity

In order to research the effects of the mounted eccentricity on the transient and steady vibration responses of the pump-turbine, three different mounted eccentricities of 0 mm, 0.1 mm and 0.2 mm were chosen. Figure 8 presents the transient periodic response of upper, lower and turbine bearings in x- and y-directions for the different mounted eccentricities.

The major discovery is that the vibration amplitudes in x-direction gradually decay to a certain value irrelevant to the mounted eccentricity changes, but the vibration amplitudes in y-direction reach local maximum and approach to a stable value. The vibration amplitudes in x-direction are larger than those in y-direction for the same mounted eccentricity. The number of periods required to enter into the stable state are nearly 200, 300 and 350 as the mounted eccentricity increases from 0 to 2 mm. This fact illustrates that the smaller mounted eccentricity is advantageous to the system’s stability.



(a) $e_m = 0\text{mm}$, $b = 2\text{mm}$, $\delta_0 = 35\text{mm}$

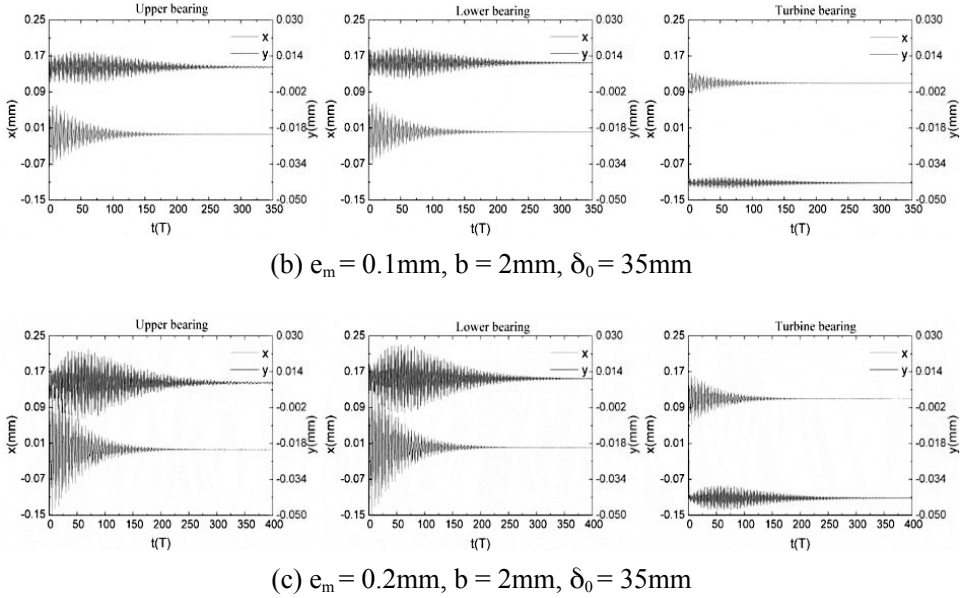


Fig. 8. The transient cycle response of three bearings with different mounted eccentricity

Figure 9 represents the stable axis orbits of three bearings for the different mounted eccentricity. The final stable axis orbits of the shaft system are the same, although the mounted eccentricities were different. But the stable vibration amplitude of the turbine bearing is larger than these for the upper and lower bearings. Therefore, the mounted eccentricity only affects the transient vibration state and don't affect the final steady vibration state.

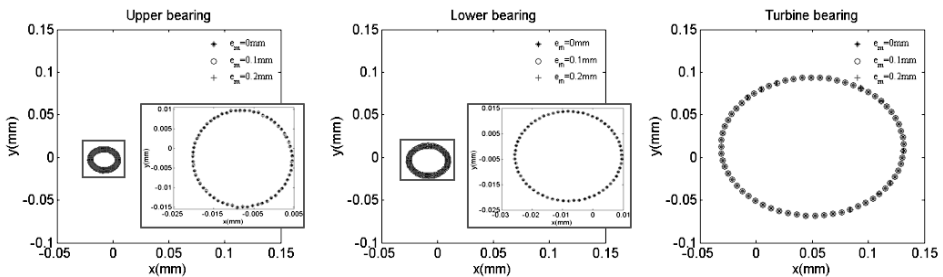
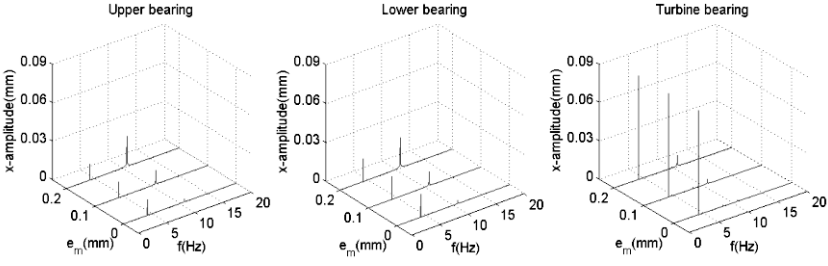
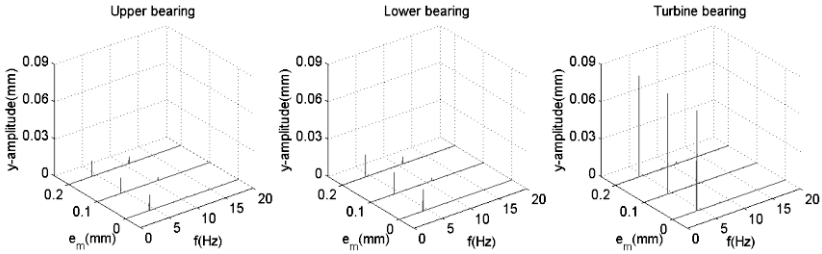


Fig. 9. The axis orbits of three bearings with different mounted eccentricity

It is evident from Figure 10 that there exists a component with frequency higher than the rotation frequency. The value of high frequency component grows as the mounted eccentricity increases. Compared with the synchronous vibration components of upper and lower bearings, the value of turbine bearing is obviously larger because the effect of thrust bearing is neglected. The high frequency component values in x-direction are larger than these in y-direction.



(a) In x-direction

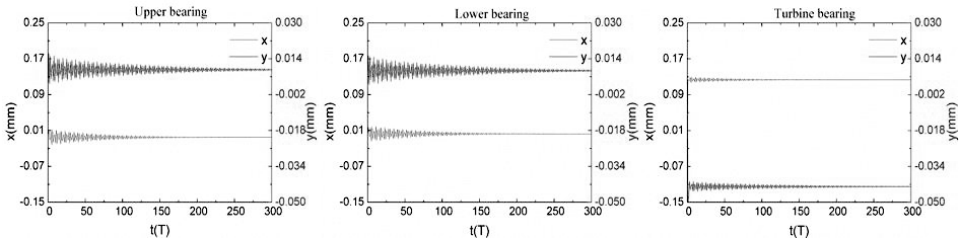


(b) In y-direction

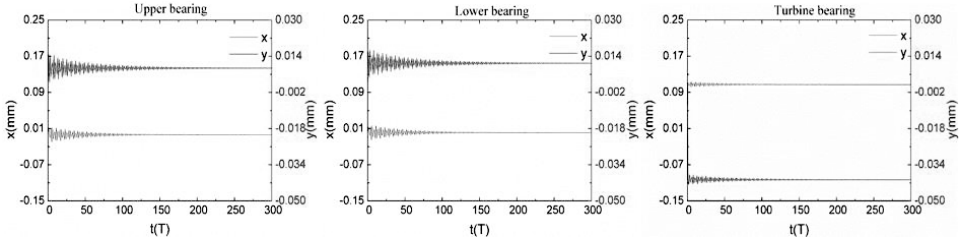
Fig. 10. The waterfall diagrams of three bearings with different mounted eccentricity

Effect of the channel clearance of crown seal

The effect of crown seal channel clearance on the vibration response of pump hydraulic turbine was also researched for three different clearances from 1 mm to 3 mm. Figure 11 presents the transient periodic response of three bearings in x- and y-direction for different crown seal channel clearance. Combining Figure 7(a) with Figure 11, it is seen that the vibration amplitudes in x- and y-direction both decrease as the periodic response times increase, and achieve a stable state. The stable values are little different for different channel clearance. Also the vibration values in both directions decay faster for larger channel clearance because the nonlinear crown sealing force weakens as the channel clearance increases.



(a) e_m = 0mm, b = 1mm, δ₀ = 35mm



(b) $e_m = 0mm, b = 3mm, \delta_0 = 35mm$

Fig. 11. The transient cycle response of three bearings with different crown seal channel clearances

In Figure 12, the stable state axis orbit vibration amplitude of the shaft system at $b = 1mm$ is significantly larger than for 2 and 3 mm. The axis orbits at $b = 2mm$ and $b = 3mm$ are nearly overlap. The main reason accounting for this phenomenon is that the F_{CS} at $b = 1mm$ is larger than these at 2mm and 3mm (as shown in Figure 6). Thus, the nonlinear sealing force has a notable influence on the dynamic vibration response of shaft system.

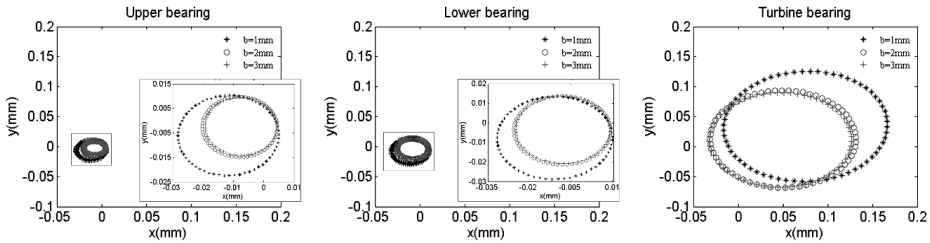


Fig. 12. The axis orbits of three bearings with different crown seal channel clearances

Figure 13 represents the waterfall diagrams of three bearings with different channel clearances in x-direction. The difference between the mounted eccentricity is in fact that there is just one isolated synchronous vibration component; in contrast, the value of high frequency component is very small. The similar frequency components are also present in the waterfall diagrams for y-direction. These calculated results are consistent with the Gong *et al.* (2013).

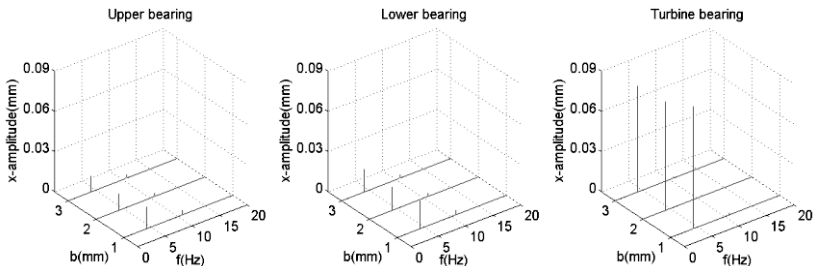


Fig. 13. The waterfall diagrams of three bearings with different crown seal channel clearances in x-direction

Effect of the air-gap length

The effect of the air-gap length on the system lateral vibration is also obvious. In order to research the effect, three different air-gap lengths ranging from 15 mm to 35 mm were chosen. Figure 14 shows the transient periodic response of three bearings in x-direction and y-direction with different air-gap length. The different air-gap length affects the vibration characteristics of the shaft system. For $\delta_0 = 15\text{mm}$, i.e. bigger UMP, the transient response decays from the distorted form, when the air-gap length increases to 25 mm. Therefore, UMP also plays significant role in the dynamic vibration of pump-turbine's shaft system.

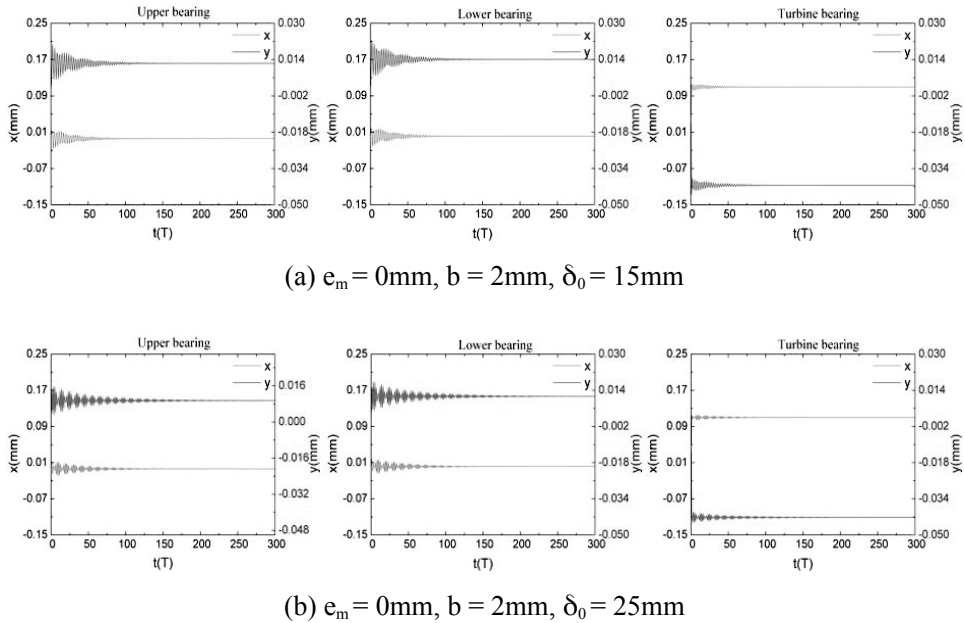


Fig. 14. The transient cycle response of three bearings to the air-gap length

The axis orbits of the upper and lower bearings (Figure 15) are similar to ones obtained for the different channel clearances. The smaller air-gap length correlates to the larger vibration amplitude. But the axis orbit of turbine's bearing remains almost unchanged as the air-gap length changes. This implies that the influences of UMP on upper bearing and lower bearing are more obvious than on the turbine bearing. In addition, all central points of the orbits are located not in the coordinate origin, which is also consistent with the actual operation situation.

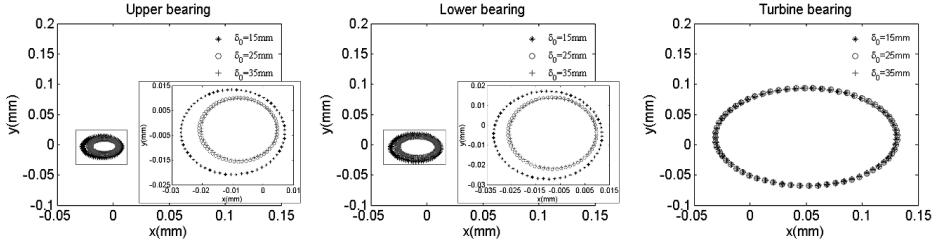


Fig. 15. The axis orbits of three bearings with different air-gap length

The vibration frequencies of three bearings with different air-gap length also contain a high frequency component and a synchronous vibration component. The changing trend of the vibration frequencies is similar to the channel clearance case.

CONCLUSIONS

The dynamic lateral vibration, including the transient vibration state and steady vibration state, of the pump-turbine's shaft system was studied in this article. The contribution of the current work can be described with the following highlights:

- (1) Crown seal force presents nonlinear changing trend with the change of channel clearance and channel length. UMP presents nonlinear changing trend with the change of air-gap length and excitation current, especially in the condition of large eccentricity ratio.
- (2) The mounted eccentricity only affects the transient vibration state and does not affect the final steady vibration state. The stability of the shaft system decreases with the increase of the mounted eccentricity.
- (3) The vibration amplitude of the system is obviously larger for $e = 1$ mm or $\delta_0 = 15$ mm, which facilitates the idea that the nonlinear F_{CS} and UMP are important to lateral vibration of the pump-turbine's shaft system.

The novel model proposed in this paper proves that the nonlinear sealing force should be taken into consideration in dynamic vibration of pump-turbine's shaft system.

ACKNOWLEDGEMENTS

This work was supported by the National Natural Science Foundation of China (Grant No. 51479167), China National Science and Technology Support Project (Grant No. 2011BAF03B01) and Science and Technology Key Project of Zhejiang Province (Grant No. 2014C01066).

REFERENCES

- Bai, B., Zhang, L., Guo, T. & Liu, C. 2012.** Analysis of dynamic characteristics of the main rotor system in a hydro-turbine based on ANSYS. *Procedia Engineering* **31**: 654-658.
- Bettig, B. P. & Han, R. P. S. 1999.** Modeling the lateral vibration of hydraulic turbine-generator rotors. *Journal of Vibration and Acoustics* **121**(3): 322-327.
- Childs, D. W. 1983.** Dynamic analysis of turbulent annular seals based on Hirs' lubrication equation. *Journal of Lubrication Technology* **105**(3): 429-436.
- De Jaeger, E., Janssens, N., Malfliet, B. & Van De Meulebroecke, F. 1994.** Hydro turbine model for system dynamic studies. *IEEE Transactions on Power Systems* **9**(4): 1709-1715.
- Feng, F. & Chu, F. 2001.** Dynamic analysis of a hydraulic turbine unit. *Mechanics of Structures and Machines* **29**(4): 505-531.
- Gong, R. Z., Wang, H. J., Liu, Q. Z., Shu, L. F. & Li, F. C. 2013.** Numerical simulation and rotor dynamic stability analysis on a large hydraulic turbine. *Computers & Fluids* **88**: 11-18.
- Gong, R. Z., Wang, H., Zhao, J. L., Li, D. Y. & Wei, X. Z. 2014.** Influence of clearance parameters on the rotor dynamic character of hydraulic turbine shaft system. *Proceedings of the Institution of Mechanical Engineers, Part C: Journal of Mechanical Engineering Science* **228**(2): 262-270.
- Guo, D., Chu, F. & Chen, D. 2002.** The unbalanced magnetic pull and its effects on vibration in a three-phase generator with eccentric rotor. *Journal of Sound and Vibration* **254**(2): 297-312.
- Lai, X. D., Liao, G. L., Zhu, Y., Zhang, X., Gou, Q. Q. & Zhang, W. B. 2012.** Lateral vibration of hydro turbine-generator rotor with varying stiffness of guide bearings. *IOP Conference Series: Earth and Environmental Science*. IOP Publishing, U.K.
- Li, J., Obi, S. & Feng, Z. 2009.** The effects of clearance sizes on labyrinth brush seal leakage performance using a Reynolds-averaged Navier—Stokes solver and non-Darcian porous medium model. *Proceedings of the Institution of Mechanical Engineers, Part A: Journal of Power and Energy* **223**(8): 953-964.
- Muszynska, A. 1988.** Improvements in lightly loaded rotor/bearing and rotor/seal models. *Journal of Vibration, Acoustics, Stress, and Reliability in Design* **110**(2): 129-136.
- Muszynska, A. 2005.** *Rotordynamics*. CRC Press, Boca Raton. Pp. 1-8.
- Muszynska, A. & Bently, D. E. 1990.** Frequency-swept rotating input perturbation techniques and identification of the fluid force models in rotor/bearing/seal systems and fluid handling machines. *Journal of Sound and Vibration* **143**(1): 103-124.
- Peng, Y. C., Chen, X. Y., Zhang, K. W. & Hou, G. X. 2007.** Numerical research on water guide bearing of hydro-generator unit using finite volume method. *Journal of Hydrodynamics, Ser. B* **19**(5): 635-642.
- Perers, R., Lundin, U. & Leijon, M. 2007.** Saturation effects on unbalanced magnetic pull in a hydroelectric generator with an eccentric rotor. *IEEE Transactions on Magnetics* **43**(10): 3884-3890.
- Scharrer, J. K. 1988.** Theory versus experiment for the rotordynamic coefficients of labyrinth Furthmoregas seals: Part I—a two control volume model. *Journal of Vibration and Acoustics* **110**(3): 270-280.
- Simmons, G. F., Cha, M., Aidanpää, J. O., Cervantes, M. J. & Glavatskih, S. 2014.** Steady state and dynamic characteristics for guide bearings of a hydro-electric unit. *Proceedings of the Institution of Mechanical Engineers, Part J: Journal of Engineering Tribology* **228**(8): 836-848.
- Wang, L. H., Wang, R. L. & Sun, W. Q. 2011.** *Vibration and Analysis of Hydrogenerator Set*. The Yellow River Water Conservancy Press, Zheng Zhou. Pp. 131-136.

- Wyssmann, H. R., Pham, T. C. & Jenny, R. J. 1984.** Prediction of stiffness and damping coefficients for centrifugal compressor labyrinth seals. *Journal of Engineering for Gas Turbines and Power* **106**(4): 920-926.
- Xu, Y. & Li, Z. 2012.** Computational model for investigating the influence of unbalanced magnetic pull on the radial vibration of large hydro-turbine generators. *Journal of Vibration and Acoustics* **134**(5): 051013.
- Xu, Y., Li, Z. & Lai, X. 2011.** Simulation model of radial vibration for a large hydro-turbine generator unit and its application. *Power Engineering and Automation Conference (PEAM), 2011 IEEE*. IEEE, USA.
- Yan, X., Li, J. & Feng, Z. 2011.** Effects of sealing clearance and stepped geometries on discharge and heat transfer characteristics of stepped labyrinth seals. *Proceedings of the Institution of Mechanical Engineers, Part A: Journal of Power and Energy* **225**(4): 521-538.
- Zhong, Y. E., He, Y. Z., Wang, Z. & Li, F. Z. 1987.** *Rotordynamics*. Tsinghua University Press, Beijing. Pp. 183-185.
- Zhou, W., Wei, X., Wei, X. & Wang, L. 2014.** Numerical analysis of a nonlinear double disc rotor-seal system. *Journal of Zhejiang University-SCIENCE A (Applied Physics & Engineering)* **15**(1): 39-52.

Submitted: 8-2-2015

Revised: 6-5-2015

Accepted: 28-6-2015